

Estimates on the possible annual seismicity of Venus

Iris van Zelst^{1,2}, Julia Maia³, Ana-Catalina Plesa¹, Richard Ghail⁴, Moritz Spühler¹

¹Institute of Planetary Research, German Aerospace Center (DLR), Berlin, Germany

²Centre of Astronomy and Astrophysics, Berlin Institute of Technology, Berlin, Germany

³Université Côte d'Azur, Observatoire de la Côte d'Azur, CNRS, Laboratoire Lagrange, Nice, France

⁴Department of Earth Sciences, Royal Holloway, University of London, Egham, UK

Key Points:

- An inactive Venus with global background seismicity like Earth's continental intraplate seismicity has a few hundred quakes $\geq M_w 4$ per year
- A lower bound on an active Venus where ridges, coronae, and rifts are seismically active predicts a few thousand quakes $\geq M_w 4$ annually
- The upper bound for an active Venus results in thousands ($\sim 5,000 - 18,000$) venusquakes $\geq M_w 4$ per year

This manuscript is a preprint which has been submitted for publication.
It has not undergone peer review yet.
Subsequent versions of this manuscript may have slightly different content.
If accepted, the final version of this manuscript will be available
via the 'Peer-reviewed Publication DOI' link on the right-hand side of this
webpage. Please feel free to contact any of the authors; we welcome
feedback!

Twitter: @iris_van_zelst

15 Abstract

16 There is a growing consensus that Venus is seismically active, although its level of seismicity could be very different from that of Earth due to the lack of plate tectonics. Here, we estimate upper and lower bounds on the expected annual seismicity of Venus by scaling the seismicity of the Earth. We consider different scaling factors for different tectonic settings and account for the lower seismogenic zone thickness of Venus. We find that 95 – 296 venusquakes $\geq M_w 4$ per year are expected for an inactive Venus, where the global seismicity rate is assumed to be similar to that of continental intraplate seismicity on Earth. For the active Venus scenarios, we assume that the coronae, ridges, and rifts of Venus are currently seismically active. This results in 1,161 – 3,609 venusquakes $\geq M_w 4$ annually as a realistic lower bound and 5,715 – 17,773 venusquakes $\geq M_w 4$ per year as a maximum upper bound for an active Venus.

27 Plain Language Summary

28 Venus could be seismically active at the moment, but it is uncertain how many earthquakes (or to use the proper term: venusquakes) there could be in a year. Here, we calculate the minimum and maximum number of venusquakes we could expect in a given year on Venus based on different assumptions. If we assume there is not much seismic activity on Venus (comparable to the interior of tectonic plates on Earth), we find that we could expect about a few hundred venusquakes per year with a magnitude bigger than or equal to 4. For an estimate of the maximum amount of venusquakes, we assume that Venus has regions with more seismic activity: the so-called coronae, ridges, and rifts. Depending on our assumptions, we then find that more than 17,000 venusquakes could occur in a year with a magnitude bigger than or equal to 4.

38 1 Introduction

39 After the successful mapping of the Venusian surface by Magellan from 1990 to 1992, for a long time the prevailing hypotheses for Venus’s geodynamic regime were that of a catastrophic or episodic resurfacing regime. Reason for this was the observation of a relatively low number of craters (932; Strom et al., 1994) on the surface, from which people deduced a uniform, relatively young surface age of 800–240 Myrs (McKinnon et al., 1997; Feuvre & Wieczorek, 2011). In these catastrophic or episodic resurfacing scenarios, Venus is currently in a relatively quiet tectonic phase after the geologically-recent resurfacing event that led to the observed young surface age (Rolf et al., 2022; O’Rourke et al., 2023).

48 In recent years, however, the view on Venus’s current tectonic activity has shifted towards a more active planet, rivalled in the Solar System only, perhaps, by our own Earth. From a geodynamical point of view, other theories for its geodynamic regime have been put forward, such as the plutonic squishy lid regime (Lourenço et al., 2020), which are consistent with ongoing activity on Venus today. Additionally, the shift towards an active Venus is partly induced by compelling evidence from Magellan, Pioneer Venus, and Venus Express data that Venus might be currently volcanically active. Data from Venus Express shows regions of high emissivity which could be associated with chemically unweathered, and therefore likely geologically young (~ 2.5 Myrs), surfaces. These anomalies correlate with volcanic highlands, such as Imdr Regio (Smrekar et al., 2010), indicating geologically recent volcanism in these regions. Later, weathering experiments under Venusian conditions indicated that the reduction of surface emissivity is a rapid process on the order of years. Filiberto et al. (2020); Brossier et al. (2022) therefore postulate that the low radar emissivity values in Ganis chasma could be the result of volcanic eruptions in the last 30 years, indicating that Venus is volcanically active now. The observed variability in SO_2 concentration in the clouds by Pioneer Venus and Venus Ex-

64 press from 1979-2011 could also be attributed to recent volcanic eruptions (Marcq et al.,
 65 2013). The most compelling evidence for active volcanism on Venus to date comes from
 66 Herrick and Hensley (2023), who observed changes in a volcanic region by analysing con-
 67 secutive radar images acquired by Magellan. They interpreted these changes as volcanic
 68 flows and hence ongoing volcanic activity on Venus. In line with that, recent estimates
 69 from scaling the volcanism of Earth to Venus yield 12 – 42 volcanic eruptions on Venus
 70 in a year, depending on assumptions on the amount of volcanism associated with plume-
 71 induced subduction at coronae (Byrne & Krishnamoorthy, 2022; Van Zelst, 2022). Fu-
 72 ture missions such as VERITAS (Smrekar et al., 2020) and EnVision (Ghail et al., 2016)
 73 will provide better constraints on Venus’s volcanic activity.

74 In the meantime, since Venus seems to be volcanically and geologically active, it
 75 is reasonable to assume that it is also seismically active. Indeed, its seismicity could be
 76 more extensive than that of Mars and the Moon, which both are believed to be signif-
 77 icantly less tectonically active than Venus (Stevenson et al., 2015). On these bodies, de-
 78 spite being in a stagnant lid regime, seismicity has been observed with the successfully
 79 deployed Apollo Lunar Surface Experiments Package on the Moon (Nakamura et al., 1982)
 80 and on Mars with the InSight mission (Banerdt et al., 2020). As Venus is now thought
 81 to be in a more tectonically active geodynamic regime than a stagnant lid (Rolf et al.,
 82 2022), its potential seismicity is thought to be at least comparable with Earth’s intraplate
 83 seismicity (Stevenson et al., 2015; Tian et al., 2023; Ganesh et al., 2023). On top of that,
 84 observed rift systems (Ivanov & Head, 2011), ridges, and coronae features linked to ac-
 85 tive subduction (Davaille et al., 2017; Gülcher et al., 2020) could be seismically active
 86 at present. There are even speculations that the Venera 14 lander recorded microseisms
 87 from far-away seismicity in the active Beta regio on Venus, although there are many other
 88 potential explanations for these recorded signals (Ksanfomaliti et al., 1982).

89 Besides a large variety of tectonic features with potential Earth analogues, the crust
 90 of Venus has properties similar to the Earth’s crust. Direct compositional measurements
 91 from the Soviet landers have shown that the surface of Venus has a similar composition
 92 to that of mid-oceanic ridge basalts on Earth (e.g., Abdrakhimov & Basilevsky, 2002).
 93 Moreover, the average crustal thickness of Venus has been estimated to be about 15 –
 94 20 km (James et al., 2013; Maia & Wiczorek, 2022), which is comparable to the thick-
 95 ness of Earth’s oceanic crust. Considering these similarities, it is reasonable to use Earth’s
 96 seismic activity as a starting point to better understand the level of seismicity expected
 97 for Venus.

98 Here, we estimate upper and lower bounds of the amount of seismicity that could
 99 be expected for an active Venus, as well as an inactive Venus with seismicity reminis-
 100 cent of intraplate seismicity on Earth. By scaling the seismicity of the Earth to Venus
 101 in Section 2 for different tectonic settings, i.e., using the same philosophy as Byrne and
 102 Krishnamoorthy (2022) that Earth analogues can be applied to Venus, we obtain our re-
 103 sults (Section 3). We discuss the assumptions in our method and the estimates of pre-
 104 vious studies in detail in Section 4. This is followed by our conclusions in Section 5.

105 2 Methods

106 In order to make estimates of the seismicity of Venus, we use a global earthquake
 107 catalogue for Earth and sort the earthquakes into different tectonic areas on the globe,
 108 thereby obtaining an effective seismicity density for each tectonic setting. We then ap-
 109 ply this same density to analogous Venusian settings to obtain three different possible
 110 estimates of Venus’s current seismicity: an estimate for an inactive Venus and an upper
 111 and lower bound for an active Venus, depending on the assumptions that we make. Here,
 112 we present our methods in detail.

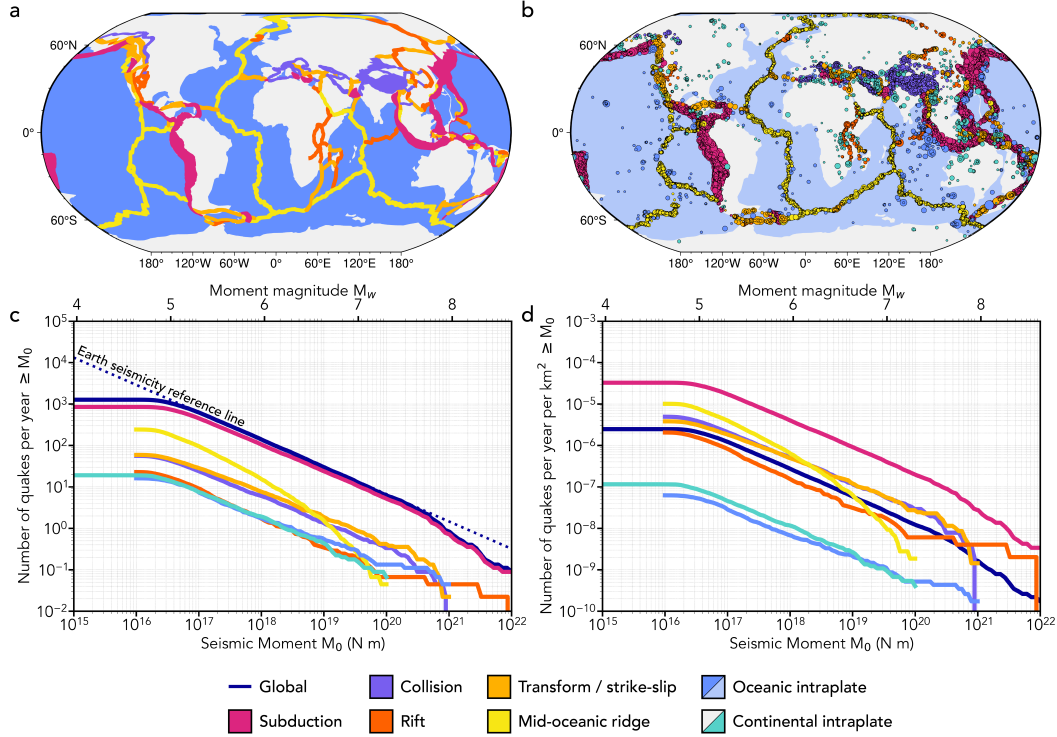


Figure 1. (a) Map of the Earth showing how its surface area is divided into seven discrete tectonic settings. (b) Earthquakes in the CMT catalogue from 1976 - 2020 coloured according to tectonic setting with the symbol size proportional to the earthquake magnitude. (c) Annual earthquake size-frequency distribution for the Earth based on the CMT catalogue and split into different tectonic settings. (d) Seismicity density on the Earth for different tectonic settings, i.e., number of earthquakes in the CMT catalogue per year per km^2 . Maps are in Robinson projection.

113

2.1 Tectonic settings on Earth

114

To obtain the seismicity density of different tectonic settings on Earth, we calculate the area of seven different tectonic settings on the Earth. For this, we use the recent maps of global geological provinces and tectonic plates from Hasterok et al. (2022). We define subduction and collision zone areas according to the zones of deformation defined by Hasterok et al. (2022), as the location of the seismicity associated with these types of plate boundaries typically encompasses a large, diffuse area. We extend the deformation zones of Hasterok et al. (2022) to account for deep earthquakes associated with subduction zones that lie outside of the deformation zones defined at the surface of the Earth. We further define the areas of transform and strike-slip regions, rift zones, and mid-oceanic ridges according to the mapping of Hasterok et al. (2022) by defining a 150 km wide band on either side of the respective plate boundary and correcting for overlapping areas. The remaining surface area of the Earth is divided into oceanic intraplate and continental intraplate regions, according to the mapped oceanic and continental crust by Hasterok et al. (2022). Hence, the surface area of the Earth is divided into seven distinct (non-overlapping) tectonic settings: subduction zones (5.13% of Earth's surface area), collision zones (2.23%), transform and strike-slip regions (3.03%), rift zones (2.17%), mid-oceanic ridges (4.70%), and oceanic (50.44%) and continental intraplate (32.30%) regions (Figure 1a, Table S1).

 129
130
131

132 2.2 Seismicity of the Earth

133 We use the global Centroid Moment Tensor (CMT) earthquake catalogue from 1976
 134 – 2020 with a completeness magnitude of $M_w 5$ to characterise Earth’s annual seismic-
 135 ity. Throughout our study, we follow Beroza and Kanamori (2015) by using the follow-
 136 ing expression to convert from seismic moment M_0 (in N m) to moment magnitude M_w :

$$\log M_0 = 1.5M_w + 9.05. \quad (1)$$

137 We sort the earthquakes of the CMT catalogue in the predefined tectonic areas (Figure 1b)
 138 and obtain an earthquake size-frequency distribution for the different tectonic settings
 139 (Figure 1c). The seismicity density for each of the tectonic settings found on Earth is
 140 then calculated by dividing the earthquake size-frequency distribution by the surface area
 141 (Figure 1d; Table S1).

142 Subduction zones have the highest seismicity density, followed by the other plate
 143 boundary settings and the overall global seismicity density of the Earth (Figure 1d). The
 144 seismicity density of collision zones and strike-slip regions are similar, with a slightly lower
 145 seismicity density for the rift zones. Intraplate seismicity clearly has the lowest seismic-
 146 ity density (approximately one order of magnitude less than the global seismicity den-
 147 sity) with continental intraplate seismicity density being slightly higher than oceanic in-
 148 traplate seismicity density.

149 2.3 Tectonic settings on Venus

150 For Venus, we consider three different tectonic settings in this study: Venusian rifts,
 151 regions characterised by compressional deformation including ridges and mountain belts,
 152 and the volcano-tectonic corona features. For each of these tectonic settings, we assign
 153 plausible, potential Earth analogues to obtain an estimate of the potential annual seis-
 154 micity of Venus. We refrain from including other tectonic settings found on Venus, such
 155 as tesserae and wrinkle ridges, as they do not have a clear Earth analogue, which makes
 156 their seismicity density unconstrained. Instead, we consider the remaining area of Venus
 157 as an intraplate tectonic setting (Figure 2a).

158 2.3.1 Rift zones

159 Rifts on Venus are typically defined as large, broad structural units of 100 km or
 160 more that are characterised by closely-spaced extensional structures (Price & Suppe, 1995;
 161 Ivanov & Head, 2011). They are similar to the so-called groove belts on Venus, which
 162 are smaller and typically contain less dense faulting patterns (Ivanov & Head, 2011). The
 163 extensional features in rift zones are often interpreted as normal faulting and horst-and-
 164 graben structures, which are typically associated with continental rifting on Earth (Foster
 165 & Nimmo, 1996). Indeed, many studies have pointed out both the morphological sim-
 166 ilarity and the similar amount of crustal extension between rifts on Venus and continen-
 167 tal rifts on Earth (e.g., McGill et al., 1981; R. Phillips et al., 1981; Stoddard & Jurdy,
 168 2012).

169 For example, Foster and Nimmo (1996) provide a detailed comparison between the
 170 East African Rift system on Earth and the rift systems of the Beta Regio on Venus. They
 171 identified many similarities, including maximum fault segment lengths, and concluded
 172 that differences stem from the lack of sediment and larger fault strength on Venus. As
 173 another example, Graff et al. (2018) suggested that the rift morphologies of Venus could
 174 be analogous to the Atlantic Rift System prior to ocean opening.

175 Modelling studies also indicate that continental rifting is a plausible mechanism
 176 to generate the rifting morphologies observed on Venus (Regorda et al., 2023). It is clear,

177 however, that the difference in surface conditions between Venus and Earth plays a role
178 in the rift mechanism as well (Regorda et al., 2023).

179 In general, the physical mechanisms governing the formation of rifts on Venus are
180 still largely unclear. Continental rifting on Earth could be a reasonable analogue for Venus,
181 especially since continental crust has been suggested for various regions on Venus (also
182 see Section 2.3.2), including the tesserae where rift-like heavily-faulted structures called
183 ‘ribbons’ can be found (Hansen & Willis, 1998; Hansen et al., 2000). However, consid-
184 ering Venus’s basaltic crustal composition — potentially more similar to Earth’s oceanic
185 crust rather than it’s continental crust (Head, 1990) — and increased surface temper-
186 ature, the rifts on Venus might also bear resemblance to the mid-oceanic ridges on Earth.
187 Although they are both extensional processes, continental rifting and mid-oceanic ridge
188 formation display quite different dynamics on Earth and consequently have different seis-
189 mic signatures (Section 2.2).

190 *2.3.2 Ridges and mountain belts on Venus*

191 There are several different types of compressional structures on the surface of Venus,
192 including ridges, ridge belts (defined as closely-clustered ridges; Frank & Head, 1990),
193 and mountain belts (Price & Suppe, 1995). These features typically resemble each other,
194 but differ in terms of topography (Ivanov & Head, 2011). The origin of these compres-
195 sional features has been debated, with early studies proposing early stage mantle down-
196 wellings as a mechanism (Zuber, 1990) and perhaps even subduction (Kryuchkov, 1990).
197 However, nowadays a continental collision mechanism is one of the most favoured inter-
198 pretations of Venus’s mountainous structures. One of the lines of evidence for this is that
199 felsic rock compositions typically associated with continental crust on Earth have been
200 suggested for tessera terrain (Mueller et al., 2008; Gilmore et al., 2015, 2017) and the
201 highlands of Venus (Hashimoto et al., 2008) based on thermal emission imaging obser-
202 vations (Smrekar et al., 2018). Hence, it has been suggested that the Ishtar Terra high-
203 lands (R. J. Phillips & Malin, 1984; Hashimoto et al., 2008) and Venus’s crustal plateaus
204 (Nikolaeva et al., 1992; Romeo & Turcotte, 2008; Romeo & Capote, 2011) are composed
205 of continental crust. The observed compressional deformation structures — and in par-
206 ticular the highlands of Venus — are therefore thought to be the result of a process sim-
207 ilar to continental collision on Earth (R. J. Phillips & Malin, 1984; Jull & Arkani-Hamed,
208 1995; Romeo & Turcotte, 2008).

209 *2.3.3 Coronae and corona-like features*

210 Coronae are roughly circular structures characterised by an annulus of high deforma-
211 tion (Price & Suppe, 1995). They are unique to Venus and are typically associated
212 with volcanism and mantle upwellings (Smrekar & Stofan, 1997). There are various to-
213 pographic signatures associated with coronae, which have been linked to differences in
214 formation mechanisms and stages of formation (Smrekar & Stofan, 1997; Gülcher et al.,
215 2020).

216 The most commonly-accepted hypothesis of corona formation nowadays is that of
217 plume-induced subduction, where a rising plume impinges on the Venusian lithosphere
218 and causes subduction-like dynamics and delamination at its edges (Gerya, 2014; Davaille
219 et al., 2017; Smrekar et al., 2018; Gülcher et al., 2020; Baes et al., 2021). For example,
220 Gülcher et al. (2020) used 3-D numerical models to show that different corona structures
221 could represent different plume styles and stages of formation. Using these modelling in-
222 sights and comparing to topographic data of Venus, Gülcher et al. (2020) found that 37
223 of 133 studied coronae (i.e., 27.8%) could be actively forming tectonic structures at present.
224 The remaining coronae that they studied were either deemed to be inactive (26.3%) or
225 inconclusive (45.9%) according to the modelled topography profiles. It is worth noting
226 that the coronae studied in Gülcher et al. (2020) are not the complete set of observed

227 coronae on Venus and are instead biased towards the larger corona structures with a di-
 228 ameter ≥ 300 km. Still, their modelling study provides compelling evidence that tec-
 229 tonic processes — and specifically subduction-like processes — in a subset of the cor-
 230 nae could still be active today.

231 **2.3.4 The surface areas of different tectonic features on Venus**

232 We calculate the surface area covered by rifts (8.25% of Venus’s surface area; Ju-
 233 rdy & Stoddard, 2007), coronae (7.76%), and ridges or mountain belts (i.e., compres-
 234 sional regions; 1.64%) from maps by Price and Suppe (1995); Price et al. (1996) as shown
 235 in Figure 2a (also see Table S2). We manually ensure that there are no overlapping re-
 236 gions by including rift-associated coronae as part of the rift system. The remaining sur-
 237 face area of Venus that is not assigned an actively-deforming tectonic setting is then con-
 238 sidered to be intraplate (82.35% of Venus’s surface; Figure 2a).

239 **2.4 Scaling from the Earth to Venus**

240 **2.4.1 Seismogenic thickness**

241 The seismogenic thickness of a planet’s lithosphere is the maximum depth at which
 242 earthquakes can nucleate, typically dictated by the temperature structure of the litho-
 243 sphere and the location of the brittle-ductile transition. On Earth, the down-dip limit
 244 of the seismogenic zone in subduction zones is for example associated with the 350°C
 245 and 450°C isotherms (Hyndman & Wang, 1993; Hyndman et al., 1997; Gutscher & Pea-
 246 cock, 2003), although the 600°C isotherm is often cited as the maximum limit for brit-
 247 tle failure, stemming from observations of intermediate-depth seismicity (Jung et al., 2004;
 248 Wang et al., 2017). Taken over the entire surface area of the planet, the seismogenic thick-
 249 ness transforms into the seismogenic volume. As a measure of seismicity, the seismogenic
 250 thickness is of limited use as it merely defines the region where quakes could nucleate
 251 and slip. Indeed, earthquakes can propagate below the seismogenic depth (although they
 252 nucleate above it) and there are — depending on tectonic setting — vast regions with
 253 a significant seismogenic thickness that experience limited seismicity, e.g. the interiors
 254 of continental plates, which typically undergo limited deformation. Despite its limita-
 255 tions, seismogenic thickness is still a useful variable to look at when determining the max-
 256 imum amount of seismicity that could occur on a given planet.

257 Since Venus has a higher surface temperature than Earth, assuming the same seis-
 258 mogenic thickness for both is likely incorrect. More specifically, we expect Venus to have
 259 a lower seismogenic thickness than Earth due to its higher surface temperature and hence
 260 shallower brittle-ductile transition in its lithosphere. We therefore need to take the likely
 261 difference in seismogenic thickness between the two planets into account when estimat-
 262 ing the seismicity of Venus.

263 In order to estimate the seismogenic thickness scaling factor between Earth and
 264 Venus, we first estimate the average seismogenic thickness for the Earth, which is rel-
 265 atively well constrained. For oceanic crust, we assume a representative seismogenic thick-
 266 ness of 36.5 km, which is the depth of the 600°C isotherm (McKenzie et al., 2005; Richards
 267 et al., 2018) for the average age of 64.2 Myrs of the oceanic crust (Seton et al., 2020).
 268 Following Wright et al. (2013), we assume a seismogenic thickness of 14 km for conti-
 269 nental crust. Then, applying the ratio of oceanic / continental crust from Hasterok et
 270 al. (2022), we obtain an average seismogenic zone thickness for the Earth of 26.93 km.

271 For Venus, we calculate a likely minimum and maximum seismogenic thickness from
 272 proposed end-member thermal gradients of Venus’s lithosphere (Smrekar et al., 2023; Bjonnes
 273 et al., 2021). Like for our Earth estimate, we calculate the depth corresponding to the
 274 600°C isotherm, as this seems to limit the seismogenic zone on Earth (McKenzie et al.,
 275 2005). To obtain a minimum estimate of Venus’s seismogenic zone thickness, we calcu-

late the average thermal gradient for Venusian rifts estimated by Smrekar et al. (2023), which results in a seismogenic thickness of 7.3 km. As a maximum estimate, we use the proposed minimum thermal gradient of 6 K/km for the Mead crater on Venus by Bjonnes et al. (2021), resulting in a seismogenic thickness of 22.7 km. We note that these estimates represent the thermal gradients during the formation of the associated features, but given the young ages predicted for Venus’s surface these values are likely representative for its current thermal state.

Combining these estimates of the Venusian seismogenic thickness with that of Earth, we obtain minimum and maximum scaling ratios of 0.27 and 0.84, respectively, to account for the likely difference in seismogenic thickness between Venus and Earth.

2.4.2 Three end-member estimates

We consider three different scenarios when scaling the seismicity from the Earth to Venus (Table S3). First, we consider an inactive Venus where the only seismicity on the planet is a background seismicity similar to the continental intraplate seismicity on Earth. This minimum level of seismicity on Venus is a popular hypothesis that has been used by other studies as well (e.g., Stevenson et al., 2015; Tian et al., 2023; Ganesh et al., 2023). Here we obtain this estimate by scaling the entirety of Venus with continental intraplate seismicity on Earth.

As a second estimate, we consider an active Venus with conservative assumptions on its level of activity to provide a lower bound. Following Davaille et al. (2017); Gülcher et al. (2020); Byrne and Krishnamoorthy (2022), we assume that coronae are surface expressions of plume-induced subduction and therefore have a seismic signature similar to that of Earth’s subduction zones. However, for this lower bound estimate, we do not consider the entire corona area to be active and associated with the high seismicity density of subduction zones. Instead, we assume that 27.8% of the area of coronae is active according to Gülcher et al. (2020) and we only scale this area with subduction zones on Earth. We further assume that the rift zones on Venus have seismicity similar to (continental) rift zones on Earth (Solomon, 1993; Foster & Nimmo, 1996; Basilevsky & McGill, 2007; Harris & Bédard, 2015; Graff et al., 2018). The observed ridges and mountain belts on Venus that result from compressional deformation are assumed to have a similar seismicity signature to collision zones on Earth. Like the inactive Venus scenario, the remaining area of Venus is scaled according to continental intraplate seismicity on Earth.

Our third and last estimate is for an active Venus with the most liberal assumptions of plausible tectonic activity on Venus. In this estimate, we assume that all coronae are active, since the amount of active coronae is still highly uncertain (Gülcher et al., 2020). So, we scale the entire corona area with the subduction seismicity of the Earth. For the rift zones on Venus, we now scale the seismicity with mid-oceanic ridge seismicity on Earth, instead of continental rifting (Graff et al., 2018). Like our lower bound estimate for active Venus, we scale the area of ridges on Venus with collision zones on Earth and we assume that the rest of the planet is equivalent to continental intraplate seismicity on Earth.

Combining the scaling for the seismogenic zone thickness (Section 2.4.1) with the three scalings based on the tectonic features allows us to arrive at three different end-member seismicity estimates for Venus. In short, we obtain the global amount of annual venusquakes for a certain magnitude $N_{\text{vq}|M_w}$ by applying the following equation:

$$N_{\text{vq}|M_w} = f_{\Delta D} \sum_{\text{tectonic features}} A_{t,V} \cdot \frac{N_{\text{eq,t}|M_w}}{A_{t,E}} \quad (2)$$

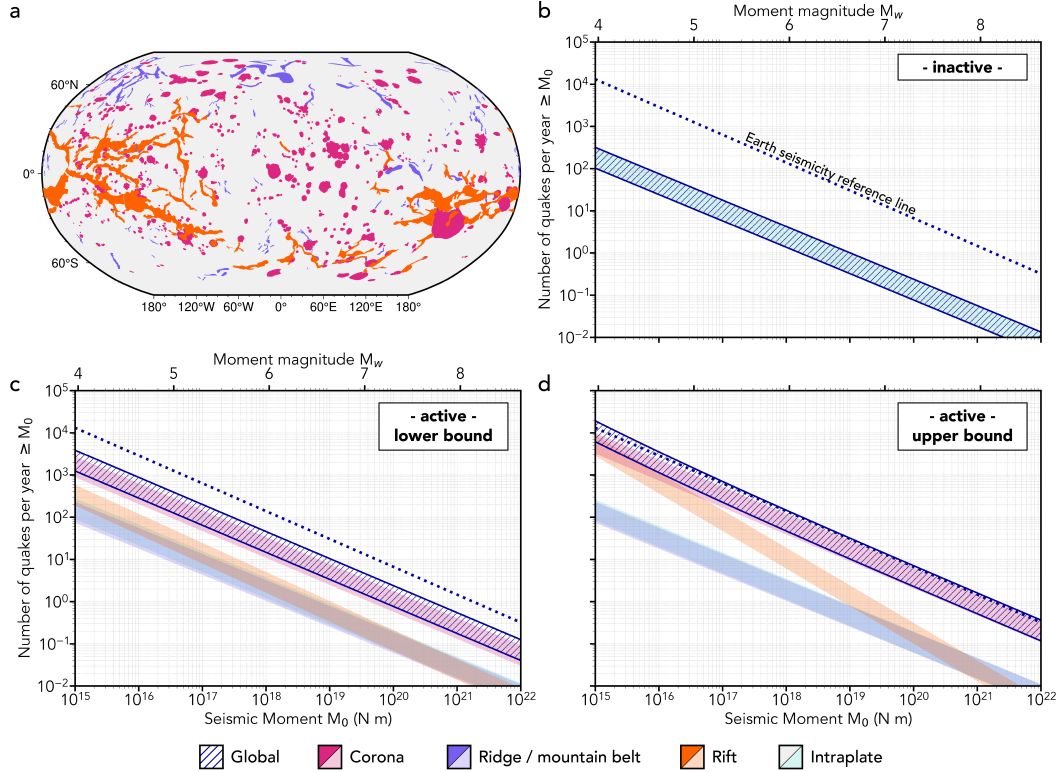


Figure 2. (a) Map of Venus (Robinson projection) showing the areas of mapped coronae, ridges and mountain belts, and rifts (Price & Suppe, 1995; Price et al., 1996). (b-d) Ranges of potential quake size-frequency distributions on Venus for (b) an inactive Venus with background seismicity analogous to Earth’s continental intraplate seismicity; (c) a lower bound on an active Venus; and (d) an upper bound on an active Venus. The hatched area shows the global, accumulated annual seismicity that combines the seismicity of the different individual tectonic settings. Note that because of the log-log scale, the global estimate and the seismicity range of the highest individual tectonic setting are closely-spaced. Dotted dark blue line indicates the reference Earth seismicity line, which corresponds with the slope of the size-frequency distribution of global seismicity on Earth (Figure 1c).

321 where $f_{\Delta D}$ is the seismogenic zone scaling factor (i.e., 0.27 and 0.84); $A_{t,V}$ is the sur-
 322 face area A of a tectonic feature t on Venus V ; $N_{\text{eq},t|M_w}$ is the number of annual earth-
 323 quakes for a given analogous Earth tectonic feature at a given moment magnitude; and
 324 $A_{t,E}$ is the corresponding surface area of the analogous tectonic feature on Earth. The
 325 sum then indicates a summation over all the tectonic features that are scaled on Venus,
 326 up to and including the intraplate regions, such that we sum over the entire surface area
 327 of Venus. Scaling with the seismogenic thickness as well as the areas of the tectonic set-
 328 tings, effectively allows us to scale by seismogenic volume per tectonic setting to obtain
 329 estimates for Venus’s seismicity (Table S3).

330 2.4.3 Extrapolating to other magnitudes

331 In order to actually calculate the potential amount of seismicity on Venus and to
 332 extrapolate to earthquake magnitudes below the completeness magnitude of $M_w 5$ of the
 333 CMT catalogue, we effectively scale the average slopes of the size-frequency distribution

for the different tectonic settings on Earth (equivalent to $N_{\text{eq,t}}$ for all moment magnitudes; Figure 1c). We specifically assume that the size-frequency distribution of medium-sized earthquakes with a seismic moment of 10^{17} Nm to 10^{19} Nm is representative for the size-frequency distribution of smaller earthquake magnitudes, i.e., the earthquakes follow Gutenberg–Richter statistics (Gutenberg & Richter, 1956; Beroza & Kanamori, 2015). This assumption allows us to provide estimates of the amount of venusquakes with moment magnitudes of M_w3 and M_w4 . We refrain from reporting on the amount of venusquakes with lower magnitudes, because they are unlikely to be detected in future seismological exploration missions of Venus (Krishnamoorthy et al., 2020; Brissaud et al., 2021).

Calculating the amount of large venusquakes with magnitudes $\geq M_w8$ is less straightforward, as the (potential) maximum quake magnitude on Venus is unknown. In addition, there is a limited amount of data for Earth on earthquakes with magnitudes $\geq M_w8$, because of their large recurrence time (Figure 1). For these reasons, we do not explicitly comment on the occurrence of quakes $\geq M_w8$ on Venus in this study, although our methodology does provide estimates (e.g., Figure 2).

3 Results

Our results for the different Venus scenarios are summarised in Figure 2 and Table 1, 2, where we list the estimated annual number of quakes for a given moment magnitude and the global seismicity densities on Venus for our different estimates.

3.1 Inactive Venus

In our first estimate, we assume that the entirety of Venus can be scaled with the continental intraplate seismicity of the Earth, so the global estimate and the intraplate estimate overlap perfectly in Figure 2b. As expected, the amount of seismicity in this scenario is significantly less than that on Earth with 95 – 296 venusquakes $\geq M_w4$ estimated annually, compared to 12,207 earthquakes $\geq M_w4$ per year on Earth. The associated seismicity density for quakes $\geq M_w4$ lies between $0.21 \cdot 10^{-6}$ and $0.64 \cdot 10^{-6}$ year $^{-1}$ km $^{-2}$ (Table 2), which is on the same order of magnitude as that of intraplate seismicity on Earth.

3.2 Active Venus - lower bound

The lower bound for our active Venus estimate globally predicts more seismicity than the inactive, intraplate Venus estimate (Section 3.1). The ridge, rift, and intraplate tectonic settings on Venus have seismicity on the same order of magnitude in this estimate, as shown by the overlapping bands of seismicity in Figure 2c (also see Figure S1). The coronae have an order of magnitude more seismicity associated with them, although only 27.8% of them are assumed to have a subduction-like seismicity density in this estimate. Summing up the seismicity of the different tectonic settings results in estimates of 1,161 – 3,609 venusquakes per year with a moment magnitude ≥ 4 and a seismicity density of $2.52 \cdot 10^{-6}$ – $7.84 \cdot 10^{-6}$ year $^{-1}$ km $^{-2}$ globally for venusquakes $\geq M_w4$ (Table 2). This global seismicity density is significantly less than that of the Earth or any of its plate boundary settings.

3.3 Active Venus - upper bound

The upper bound of estimated seismicity for an active Venus (Figures 2d, S2) is very close to – and even slightly larger than – the annual seismicity observed on Earth, primarily due to the scaling of coronae with Earth’s subduction zone seismicity in this estimate, which also dominates Earth’s seismicity (Figure 1c). Since we scale the rifts on Venus with Earth’s mid-oceanic ridge seismicity in this estimate, we have a different

Estimate	$M_w \geq 3.0$	$M_w \geq 4.0$	$M_w \geq 5.0$	$M_w \geq 6.0$	$M_w \geq 7.0$
Inactive Venus	826 - 2568	95 - 296	11 - 34	1 - 4	0 - 0
Active Venus - lower bound	10760 - 33460	1161 - 3609	126 - 391	14 - 42	2 - 5
Active Venus - upper bound	84263 - 262023	5715 - 17773	465 - 1446	44 - 136	4 - 15

Table 1. Number of venusquakes per year equal to or larger than a certain moment magnitude for our three possible Venus scenarios. A range is provided based on the uncertainties in the chosen scaling factor for the seismogenic thickness.

380 slope for Venusian rift seismicity. This results in an increase in smaller quakes with $M_w \leq$
381 5. There is no difference between the seismicity expected for the ridge tectonic setting
382 compared to the lower bound for an active Venus (Section 3.2), as it is scaled in the same
383 way.

384 Globally, we then estimate 5,715 – 17,773 venusquakes of moment magnitude ≥ 4 ,
385 with the upper bound being larger than the number of $M_w \geq 4$ earthquakes estimated
386 for the Earth (12,207). The seismicity density of quakes $M_w \geq 4$ varies from $12.42 \cdot 10^{-6}$
387 to $38.62 \cdot 10^{-6} \text{ year}^{-1} \text{ km}^{-2}$ (Table 2). This lowest possible seismicity density for an up-
388 per bound to our active Venus estimate is slightly lower than the Earth’s seismicity den-
389 sity for continental rift zones ($16.98 \cdot 10^{-6} \text{ year}^{-1} \text{ km}^{-2}$) and the highest possible seis-
390 micity density is larger than that of the seismicity density of collision settings on the Earth
391 ($33.62 \cdot 10^{-6} \text{ year}^{-1} \text{ km}^{-2}$) (Table S1).

392 4 Discussion

393 In this study, we provide three end-member estimates of possible Venusian seismic-
394 ity by looking at Earth analogues, following the same philosophy of Byrne and Krish-
395 namoorthy (2022) who previously applied this logic to determine the frequency of vol-
396 canic eruptions on Venus. In contrast to Byrne and Krishnamoorthy (2022), we calcu-
397 late the seismic densities for individual tectonic settings and then scale according to their
398 surface areas and appropriate Earth analogues.

399 Generally, we estimate that the seismicity of Venus is lower than that of the Earth,
400 except for the most active end-member of Venus activity. Indeed, there are large differ-
401 ences between the various estimates, indicating a range of possible seismic activity on
402 Venus at present, depending on the many assumptions we are forced to make given the
403 limited amount of data from Venus.

404 4.1 Likely causes of differences between the seismicity on Earth and Venus

405 Before we assess the individual assumptions we made to obtain our different esti-
406 mates of Venusian seismicity, it is useful to assess the overarching assumption that Earth’s
407 seismicity can be scaled to Venus.

408 One of the biggest and most straightforward differences between the Earth and Venus
409 is their different surface temperatures. Since temperature plays a crucial role in seismic-
410 ity through its control on the brittle-ductile transition (Tichelaar & Ruff, 1993; Hynd-
411 man et al., 1997; Peacock & Hyndman, 1999; Gutscher & Peacock, 2003; Scholz, 2019),
412 it will have a large effect on the amount of seismicity that can occur. On a global scale,
413 different surface temperatures can result in different tectonic regimes and deformation
414 mechanisms (Lenardic et al., 2008; Foley et al., 2012; Weller et al., 2015) which could
415 greatly change the seismic signatures. In its most extreme case some studies argue that
416 there will be little to no seismicity on Venus, at least at higher magnitudes (e.g., Karato

Tectonic setting	Minimum seismicity density ($\cdot 10^{-6}$ year $^{-1}$ km $^{-2}$)	Maximum seismicity density ($\cdot 10^{-6}$ year $^{-1}$ km $^{-2}$)
Inactive Venus	0.21	0.64
Active Venus - lower bound	2.52	7.84
Active Venus - upper bound	12.42	38.62

Table 2. Estimated minimum and maximum seismicity densities on Venus for quakes $\geq M_w 4$ for three scenarios with different activity-level assumptions.

417 & Barbot, 2018). These studies argue that the high surface temperatures on Venus may
 418 exclude the possibility of any kind of substantial seismogenic zone and the unstable slip
 419 mechanisms responsible for earthquakes. Instead, the stresses that are built up in the
 420 Venusian lithosphere could be released through aseismic processes, such as creep. How-
 421 ever, some of the assumptions in Karato and Barbot (2018) are unrealistically conser-
 422 vative (e.g., a global crustal thickness of 40 km; a seismogenic zone limit at 400°C) and
 423 not applicable to Venus. In our estimates, we have taken the difference in surface tem-
 424 peratures and its effect on seismicity into account through scaling end-member estimates
 425 of the seismogenic thickness of Venus with the average seismogenic thickness of Earth.
 426 While not a perfect solution encapsulating the complexity of the effect of increased sur-
 427 face temperatures, this at least forms a first approximation to take this difference into
 428 account.

429 Another important difference between Venus and Earth is likely to be the amount
 430 of water available in the crust. On Earth, water plays a vital role, especially in subduc-
 431 tion seismicity, with the pore-fluid pressure crucial in determining the stresses in megath-
 432 rust settings (Seno, 2009; Angiboust et al., 2012) and dehydration reactions responsi-
 433 ble for intermediate-depth and deep seismicity in subduction zones (Green & Houston,
 434 1995; Hacker et al., 2003; Jung et al., 2004; Houston, 2015; Wang et al., 2017). This wa-
 435 ter is typically added to the subduction system at the outer rise that underlies an ocean
 436 in subduction zones (Boneh et al., 2019). On Venus, the amount of water in the litho-
 437 sphere is relatively unconstrained (Gillmann et al., 2022; Rolf et al., 2022), with some
 438 studies suggesting that Venus is currently relatively dry (Grinspoon, 1993; Namiki & Solomon,
 439 1998; Smrekar & Sotin, 2012; Salvador et al., 2022), while others argue that there might
 440 still be a significant amount of water in Venus’s mantle (Gillmann et al., 2022). This makes
 441 it highly uncertain how big a role water could play in the seismicity of Venus. Our es-
 442 timates encompass the full spectrum of possible seismicity on Venus with our lower bound
 443 using Earth’s intraplate seismicity, where water likely plays a smaller role, and our up-
 444 per bound including subduction seismicity, where water is an important factor.

445 Strain rates play an important role in seismicity as well, because they determine
 446 the time scale of stress build-up and the recurrence time of earthquakes. On Venus, strain
 447 rates similar to Earth’s active margins have been suggested by Grimm (1994). However,
 448 due to the lack of Earth-like plate tectonics and plate boundaries, there are overall po-
 449 tentially less large rupture areas, leading to less large-magnitude quakes on Venus. The
 450 decreased seismogenic thickness of Venus also plays a role in this by limiting the max-
 451 imum rupture area. Although our estimates provide a range of potential venusquakes
 452 at large magnitudes (Table 1), it is therefore uncertain if large venusquakes could actu-
 453 ally occur. Preliminary mission designs suggest that quake magnitudes of $M_w \geq 3$ could
 454 be feasibly observed by a range of plausible seismic detection methods (Krishnamoorthy
 455 et al., 2020; Brissaud et al., 2021) and our estimates are likely most plausible for this range
 456 of seismic magnitude $3 \leq M_w \leq 5$.

457 All in all, there are many uncertainties when it comes to estimating the seismic-
 458 ity of Venus from Earth’s seismicity. Higher resolution data and missions focused on ob-
 459 serving seismicity (discussed in Section 4.3) will help to obtain seismicity estimates for
 460 Venus independent of Earth. However, since those constraints are not yet available, scal-
 461 ing the seismicity of the Earth is a reasonable first-order approximation to gain some in-
 462 sights into the potential seismicity of Venus.

463 4.2 Assumptions in and limitations of our seismicity estimates

464 For our inactive Venus estimate, we assume that the global background seismic-
 465 ity of Venus is similar to the continental intraplate seismicity of the Earth. This is a com-
 466 mon assumption that has also been suggested by e.g., Lorenz (2012); Stevenson et al.
 467 (2015); Byrne et al. (2021); Tian et al. (2023). The number of venusquakes $\geq M_w 4$ per
 468 year for this estimate (95 – 296) is also the same order of magnitude as the estimate of
 469 Ganesh et al. (2023), who calculate an estimate of Venus’s seismicity based on the cool-
 470 ing of the planet and the corresponding contraction of the lithosphere and thereby pre-
 471 dict ~ 265 venusquakes $\geq M_w 4$ per year.

472 For our estimates for an active Venus, we scale the areas of compressional defor-
 473 mation on Venus, i.e., the ridges and mountain belts, with the seismicity of collision zones
 474 on Earth. We believe this to be a reasonable assumption, considering that Venus’s ridges
 475 and the Earth analogue are both compressional regimes and continental crust and col-
 476 lision has been previously suggested for the Venusian highlands. The rifts on Venus are
 477 scaled with continental rift seismicity on Earth in the lower bound estimate for an ac-
 478 tive Venus. This is also a reasonable assumption, with many studies pointing to the mor-
 479 phological and geological similarities between the rift zones on Venus and continental rifts
 480 on Earth such as the East African rift zone (Solomon, 1993; Foster & Nimmo, 1996; Kiefer
 481 & Swafford, 2006; Basilevsky & McGill, 2007; Stoddard & Jurdy, 2012; Graff et al., 2018;
 482 Regorda et al., 2023). For our upper bound, we scale the rift zones of Venus with mid-
 483 oceanic ridge seismicity since it is also an extensional setting and the higher tempera-
 484 tures at the mid-oceanic ridges and the corresponding different slope of the size-frequency
 485 distribution on Earth might be a better fit for rift seismicity under Venus’s high surface
 486 temperature. On Earth, the different seismic signatures between continental rifts and
 487 mid-oceanic ridges is not purely temperature-related. Instead, the inherent tectonic dif-
 488 ferences between the two settings plays a role as well. Since it is unclear which of these
 489 two physical mechanisms (or their seismic signatures) best represents the rifting processes
 490 of Venus, we believe using one of them in the lower bound estimate and one in the up-
 491 per bound estimate catches the uncertainty in governing mechanisms in our estimates.
 492 For the coronae, we scale with subduction, since multiple studies suggest that coronae
 493 are the surface expressions of plume-induced subduction (Davaille et al., 2017; Gülcher
 494 et al., 2020; Byrne & Krishnamoorthy, 2022). However, the seismicity associated with
 495 this type of plume-induced subduction is uncertain. Assigning the same seismicity den-
 496 sity as regular subduction processes on Earth is a reasonable first-order approximation
 497 in the absence of other constraints, although the presumable lack of water in coronae and
 498 the higher surface temperature will certainly affect its seismic signature as well. Future
 499 modelling studies that combine geodynamic modelling with seismic cycle modelling and
 500 dynamic ruptures (e.g., van Dinther, Gerya, Dalguer, Mai, et al., 2013; van Dinther, Gerya,
 501 Dalguer, Corbi, et al., 2013; van Dinther et al., 2014; Van Zelst et al., 2019) are needed
 502 to assess the seismic signatures that could be expected at Venusian coronae. In the in-
 503 terest of providing an upper and lower bound, scaling the coronae by activity is a good
 504 first order approximation. However, it is also possible that coronae seismicity does not
 505 scale with Earth’s subduction seismicity, but is instead more analogous to, for example,
 506 transform fault seismicity related to the observed fracture zones at the rims of coronae.
 507 In general though, our upper bound for Venusian seismicity results in seismicity levels
 508 slightly higher than, but similar to, that of the Earth, which has also already been sug-
 509 gested previously (e.g., Lorenz, 2012). Choosing a different seismic density for coronae,

510 such as that of the transform fault setting, would result in a lower amount of estimated
 511 venusquakes. Since we are attempting to provide an upper limit to the possible amount
 512 of annual venusquakes, our assumption of a subduction seismic density is reasonable.

513 Apart from the uncertainty in scaling the chosen tectonic settings correctly, there
 514 are also tectonic settings on Venus that we neglect to scale explicitly. For example, we
 515 do not explicitly scale the tesserae of Venus with a tectonic setting on Earth, although
 516 they are implicitly scaled with the background intracontinental seismicity of the Earth.
 517 This is arguably one of the most reasonable assumptions for tesserae, considering that
 518 prevailing hypotheses include that they are continental crust analogues (Romeo & Tur-
 519 cotte, 2008; Gilmore et al., 2015). We also do not consider the observed extensive regions
 520 of wrinkle ridges as seismically active beyond the background intracontinental seismic-
 521 ity of the Earth. A recent study by Sabbeth et al. (2023a) presented a conservative es-
 522 timate of $9.1 \cdot 10^{16}$ N m to $5.1 \cdot 10^{17}$ N m per year for the annual moment release for
 523 wrinkle ridges on Venus based on (low-resolution) mapped fault lengths. Assuming a max-
 524 imum quake size on Venus of $M_w 4$, this translates to 81 to 455 wrinkle ridge quakes $M_w \leq$
 525 4 on Venus per year. This is a similar amount of $M_w \leq 4$ quakes as predicted for the
 526 intraplate, ridge, and rift settings in our three different estimates ranging from inactive
 527 to active. The upper bound of 455 wrinkle ridge quakes is higher than the seismicity ex-
 528 pected from the inactive Venus estimate that only considers an intraplate setting, indi-
 529 cating that our active Venus estimates are more appropriate when considering observed
 530 faulting patterns on Venus.

531 Note that in the estimates presented here, only one type of seismic source is con-
 532 sidered, i.e. earthquakes, which by definition are associated with tectonics and volcan-
 533 ism. Other sources such as landslides (Pavri et al., 1992; M. Bulmer & Guest, 1996; M. Bul-
 534 mer et al., 2006; M. H. K. Bulmer, 2012; Hahn & Byrne, 2023) could be responsible for
 535 seismic signals on Venus as well.

536 4.3 Determining the actual seismicity of Venus in the future

537 In the next decade, VERITAS (Smrekar et al., 2020) and EnVision (Ghail et al.,
 538 2016) will provide a wealth of new data, including high resolution topography, that will
 539 provide better constraints on the actual lengths, offsets, and displacements of Venusian
 540 faults. This will provide another basis of estimating Venus’s seismicity through scaling
 541 relationships applied to surface fault observations (Sabbeth et al., 2023a, 2023b).

542 The new Venus missions will also indirectly provide stronger constraints on the seis-
 543 mogenic thickness, which is typically deduced from thermal gradients estimated from stud-
 544 ies of the elastic and mechanical lithosphere thickness (e.g. Anderson & Smrekar, 2006;
 545 Borrelli et al., 2021; Maia & Wiczorek, 2022; Smrekar et al., 2023) or from impact crater
 546 modeling (Bjonnes et al., 2021). These studies rely on the analysis of gravity and topog-
 547 raphy data, for which a higher resolution will become available from the VERITAS (Smrekar
 548 et al., 2020) and EnVision (Ghail et al., 2016) missions. Estimates of the thermal gra-
 549 dient and associated seismogenic thickness could then be obtained with a higher accu-
 550 racy and on a more global scale than currently available. They could be included in fu-
 551 ture studies of seismicity on Venus and improve on the estimates presented here.

552 Until the era of new Venus data, we are unfortunately limited by the currently-available
 553 data of Venus. The simplest, first-order estimate of the seismicity of Venus is therefore
 554 obtained here through scaling Earth analogues to Venus, without considering individ-
 555 ual fault lengths or displacements and detailed seismogenic thickness estimates and in-
 556 stead uses the seismicity density characteristics of different tectonic settings on Earth.

557 To distinguish between the different scenarios presented in this study and deter-
 558 mine how seismically active Venus is, a seismological or geophysical mission to Venus is
 559 required to measure seismic signals. Although the NASA- and ESA-selected missions to

560 Venus currently do not focus on this, there are promising proposals to measure Venus’s
 561 seismicity in the not-too-distant future. For example, Kremic et al. (2020) presented a
 562 mission proposal for a long-duration Venus lander with a seismometer on board that can
 563 withstand Venus’s high surface temperature. In addition, recent advances in the balloon-
 564 detection of earthquakes show great promise for applications to Venus (Garcia et al., 2022;
 565 Krishnamoorthy & Bowman, 2023). Our estimates for Venusian seismicity may help guide
 566 the design of these missions.

567 **5 Conclusions**

568 We estimate upper and lower bounds on the expected annual seismicity of Venus
 569 by scaling the seismicity of the Earth to Venus according to the surface area of differ-
 570 ent tectonic settings and the difference in seismogenic thickness between the two plan-
 571 ets. Our most conservative estimate is an ‘inactive Venus’, where we assume the global
 572 seismicity of Venus is comparable to Earth’s continental intraplate seismicity. This re-
 573 sults in 95 – 296 venusquakes $\geq M_w 4$ per year depending on the assumption of seismo-
 574 genic zone thickness. For our active Venus scenarios, we assume that the rifts, ridges,
 575 and coronae on Venus are seismically active. For a lower bound on an active Venus, we
 576 then find 1,161 – 3,609 venusquakes $\geq M_w 4$ annually, which increases to 5,715 – 17,773
 577 venusquakes $\geq M_w 4$ for assumptions that constitute our most active Venus scenario.
 578 This latter scenario is slightly larger than the seismic activity level of the Earth. Future
 579 seismological and geophysical missions could measure the actual seismicity of Venus and
 580 distinguish between our three proposed end-members of Venusian seismic activity.

581 **Acknowledgements**

582 This research is supported by the International Space Science Institute (ISSI) in
 583 Bern, Switzerland through ISSI International Team project #566: Seismicity on Venus:
 584 Prediction & Detection. The authors warmly thank the entire ISSI team for fruitful dis-
 585 cussions and feedback. IvZ, JM, ACP, and MS additionally acknowledge the financial
 586 support and endorsement from the DLR Management Board Young Research Group Leader
 587 Program and the Executive Board Member for Space Research and Technology. IvZ also
 588 gratefully acknowledges the support by the Deutsche Forschungsgemeinschaft (DFG, Ger-
 589 man Research Foundation), Project-ID 263649064 - TRR 170.

590 **Author contribution statement**

591 Conceptualization: Iris van Zelst

592 Data curation: Julia Maia, Richard Ghail, Moritz Spühler

593 Formal Analysis: Iris van Zelst, Julia Maia

594 Funding acquisition: Iris van Zelst, Ana-Catalina Plesa

595 Methodology: Iris van Zelst, Richard Ghail

596 Supervision: Iris van Zelst

597 Visualization: Iris van Zelst, Julia Maia

598 Writing – original draft: Iris van Zelst

599 Writing – review & editing: Iris van Zelst, Julia Maia, Richard Ghail, Ana-Catalina
 600 Plesa, Moritz Spühler

Data availability statement

The Jupyter Notebooks used to make the results and plot the figures as well as the CMT database and geospatial vector data (shapefiles) of the tectonic setting areas on Earth can be found in *zenodo link to be finalised upon acceptance. For now the data is included as a zip file for the reviewer's convenience.* Explanation of individual files in this repository and additional figures and tables are provided in the Supplementary Material. Figures were made with Python and Adobe Illustrator. We used the colorblind friendly color map from the IBM Design Library (David Nichols, 2022; retrieved: February 16, 2023).

References

- Abdrakhimov, A., & Basilevsky, A. (2002). Geology of the Venera and Vega landing-site regions. *Solar System Research*, *36*, 136–159.
- Anderson, F. S., & Smrekar, S. E. (2006). Global mapping of crustal and lithospheric thickness on Venus. *Journal of Geophysical Research: Planets (1991–2012)*, *111*(E8).
- Angiboust, S., Wolf, S., Burov, E., Agard, P., & Yamato, P. (2012). Effect of fluid circulation on subduction interface tectonic processes: Insights from thermo-mechanical numerical modelling. *Earth and Planetary Science Letters*, *357*, 238–248.
- Baes, M., Stern, R. J., Whattam, S., Gerya, T. V., & Sobolev, S. V. (2021). Plume-induced subduction initiation: Revisiting models and observations. *Frontiers in Earth Science*, *9*, 766604.
- Banerdt, W. B., Smrekar, S. E., Banfield, D., Giardini, D., Golombek, M., Johnson, C. L., ... others (2020). Initial results from the InSight mission on Mars. *Nature Geoscience*, *13*(3), 183–189.
- Basilevsky, A. T., & McGill, G. E. (2007). Surface evolution of Venus. *Exploring Venus as a terrestrial planet*, *176*, 23–43.
- Beroza, G., & Kanamori, H. (2015). 4.01 - Earthquake Seismology: An Introduction and Overview. In G. Schubert (Ed.), *Treatise on geophysics* (Second ed., p. 1 - 50). Oxford: Elsevier.
- Bjonnes, E., Johnson, B., & Evans, A. (2021). Estimating Venusian thermal conditions using multiring basin morphology. *Nature Astronomy*, *5*(5), 498–502.
- Boneh, Y., Schottenfels, E., Kwong, K., Van Zelst, I., Tong, X., Eimer, M., ... Zhan, Z. (2019). Intermediate-depth earthquakes controlled by incoming plate hydration along bending-related faults. *Geophysical Research Letters*, *46*(7), 3688–3697. Retrieved from <https://agupubs.onlinelibrary.wiley.com/doi/abs/10.1029/2018GL081585> doi: 10.1029/2018GL081585
- Borrelli, M. E., O'Rourke, J. G., Smrekar, S. E., & Ostberg, C. M. (2021). A Global Survey of Lithospheric Flexure at Steep-Sided Domical Volcanoes on Venus Reveals Intermediate Elastic Thicknesses. *Journal of Geophysical Research: Planets*, *126*(7), e2020JE006756.
- Brissaud, Q., Krishnamoorthy, S., Jackson, J. M., Bowman, D. C., Komjathy, A., Cutts, J. A., ... Walsh, G. J. (2021). The first detection of an earthquake from a balloon using its acoustic signature. *Geophysical Research Letters*, *48*(12), e2021GL093013.
- Brossier, J., Gilmore, M. S., & Head, J. W. (2022). Extended Rift-Associated Volcanism in Ganis Chasma, Venus Detected From Magellan Radar Emissivity. *Geophysical Research Letters*, *49*(15), e2022GL099765.
- Bulmer, M., & Guest, J. (1996). Modified volcanic domes and associated debris aprons on Venus. *Geological Society, London, Special Publications*, *110*(1), 349–371.
- Bulmer, M., Petley, D., Murphy, W., & Mantovani, F. (2006). Detecting slope de-

- 653 formation using two-pass differential interferometry: Implications for landslide
 654 studies on Earth and other planetary bodies. *Journal of Geophysical Research:*
 655 *Planets*, 111(E6).
- 656 Bulmer, M. H. K. (2012). Landslides on other planets. In J. J. Clague & D. Stead
 657 (Eds.), *Landslides: Types, mechanisms and modeling* (p. 393–408). Cambridge
 658 University Press. doi: 10.1017/CBO9780511740367.033
- 659 Byrne, P. K., Ghail, R. C., Şengör, A. C., James, P. B., Klimczak, C., & Solomon,
 660 S. C. (2021). A globally fragmented and mobile lithosphere on Venus. *Proceed-*
 661 *ings of the National Academy of Sciences*, 118(26).
- 662 Byrne, P. K., & Krishnamoorthy, S. (2022). Estimates on the frequency of vol-
 663 canic eruptions on Venus. *Journal of Geophysical Research: Planets*, 127(1),
 664 e2021JE007040. doi: 10.1029/2021JE007040
- 665 Davaille, A., Smrekar, S. E., & Tomlinson, S. (2017). Experimental and observa-
 666 tional evidence for plume-induced subduction on Venus. *Nature Geoscience*,
 667 10(5), 349–355.
- 668 David Nichols. (2022; retrieved: February 16, 2023). *Coloring for Colorblindness*.
 669 (<http://tsitsul.in/blog/coloropt/>)
- 670 Feuvre, M. L., & Wieczorek, M. A. (2011). Nonuniform cratering of the Moon and
 671 a revised crater chronology of the inner Solar System. *Icarus*, 214(1), 1–20.
 672 Retrieved from <https://doi.org/10.1016/j.icarus.2011.03.010> doi:
 673 10.1016/j.icarus.2011.03.010
- 674 Filiberto, J., Trang, D., Treiman, A. H., & Gilmore, M. S. (2020). Present-day
 675 volcanism on Venus as evidenced from weathering rates of olivine. *Science Ad-*
 676 *vances*, 6(1), eaax7445.
- 677 Foley, B. J., Bercovici, D., & Landuyt, W. (2012). The conditions for plate tecton-
 678 ics on super-earths: inferences from convection models with damage. *Earth and*
 679 *Planetary Science Letters*, 331, 281–290.
- 680 Foster, A., & Nimmo, F. (1996). Comparisons between the rift systems of East
 681 Africa, Earth and Beta Regio, Venus. *Earth and Planetary Science Letters*,
 682 143(1-4), 183–195. doi: 10.1016/0012-821X(96)00146-X
- 683 Frank, S. L., & Head, J. W. (1990). Ridge belts on venus: Morphology and origin.
 684 *Earth, Moon, and Planets*, 50, 421–470.
- 685 Ganesh, I., Herrick, R. R., & Kremic, T. (2023). Bounds on Venus’s seismicity from
 686 theoretical and analog estimations. In *LPSC Abstracts, No. 2806*.
- 687 Garcia, R. F., Klotz, A., Hertzog, A., Martin, R., G erier, S., Kassarian, E., . . .
 688 Mimoun, D. (2022). Infrasound from large earthquakes recorded on a net-
 689 work of balloons in the stratosphere. *Geophysical Research Letters*, 49(15),
 690 e2022GL098844.
- 691 Gerya, T. V. (2014). Plume-induced crustal convection: 3d thermomechanical model
 692 and implications for the origin of novae and coronae on venus. *Earth and Plan-*
 693 *etary Science Letters*, 391, 183–192.
- 694 Ghail, R., Wilson, C. F., & Widemann, T. (2016). EnVision M5 Venus or-
 695 biter proposal: Opportunities and challenges. In *Aas/division for plane-*
 696 *tary sciences meeting abstracts# 48* (Vol. 48, pp. 216–08). doi: [https://](https://ui.adsabs.harvard.edu/abs/2016DPS....4821608G)
 697 ui.adsabs.harvard.edu/abs/2016DPS....4821608G
- 698 Gillmann, C., Way, M. J., Avice, G., Breuer, D., Golabek, G. J., H oning, D., . . .
 699 others (2022). The long-term evolution of the atmosphere of venus: Processes
 700 and feedback mechanisms: Interior-exterior exchanges. *Space Science Reviews*,
 701 218(7), 56.
- 702 Gilmore, M., Mueller, N., & Helbert, J. (2015). VIRTIS emissivity of Alpha Re-
 703 gio, Venus, with implications for tessera composition. *Icarus*, 254, 350–361.
 704 Retrieved from <https://doi.org/10.1016/j.icarus.2015.04.008> doi:
 705 10.1016/j.icarus.2015.04.008
- 706 Gilmore, M., Treiman, A., Helbert, J., & Smrekar, S. (2017). Venus surface compo-
 707 sition constrained by observation and experiment. *Space Science Reviews*, 212,

- 1511–1540.
- 708
709 Graff, J., Ernst, R. E., & Samson, C. (2018). Evidence for triple-junction rifting
710 focussed on local magmatic centres along Parga Chasma, Venus. *Icarus*, *306*,
711 122–138.
- 712 Green, H. W., & Houston, H. (1995). The mechanics of deep earthquakes. *Annual*
713 *Review of Earth and Planetary Sciences*, *23*(1), 169–213.
- 714 Grimm, R. E. (1994). Recent deformation rates on venus. *Journal of Geophysical*
715 *Research: Planets*, *99*(E11), 23163–23171.
- 716 Grinspoon, D. H. (1993). Implications of the high d/h ratio for the sources of water
717 in venus’ atmosphere. *Nature*, *363*(6428), 428–431.
- 718 Gülcher, A. J., Gerya, T. V., Montési, L. G., & Munch, J. (2020). Corona struc-
719 tures driven by plume–lithosphere interactions and evidence for ongoing plume
720 activity on Venus. *Nature Geoscience*, *13*(8), 547–554.
- 721 Gutenberg, B., & Richter, C. F. (1956). Magnitude and energy of earthquakes. *An-*
722 *nals of Geophysics*, *9*(1), 1–15.
- 723 Gutscher, M.-A., & Peacock, S. M. (2003). Thermal models of flat subduction and
724 the rupture zone of great subduction earthquakes. *Journal of Geophysical Re-*
725 *search: Solid Earth*, *108*(B1), ESE–2.
- 726 Hacker, B. R., Peacock, S. M., Abers, G. A., & Holloway, S. D. (2003). Subduction
727 factory 2. Are intermediate-depth earthquakes in subducting slabs linked to
728 metamorphic dehydration reactions? *Journal of Geophysical Research: Solid*
729 *Earth*, *108*(B1).
- 730 Hahn, R., & Byrne, P. (2023). Characterizing Styles of Volcano Gravitational Deform-
731 ation On Venus. In *Lunar and planetary science conference abstracts 2023*.
- 732 Hansen, V. L., Phillips, R. J., Willis, J. J., & Ghent, R. R. (2000). Structures in
733 tessera terrain, Venus: Issues and answers. *Journal of Geophysical Research:*
734 *Planets*, *105*(E2), 4135–4152.
- 735 Hansen, V. L., & Willis, J. J. (1998). Ribbon terrain formation, southwestern For-
736 tuna Tessera, Venus: Implications for lithosphere evolution. *Icarus*, *132*(2),
737 321–343.
- 738 Harris, L. B., & Bédard, J. H. (2015). Interactions between continent-like ‘drift’,
739 rifting and mantle flow on venus: gravity interpretations and earth analogues.
740 *Geological Society, London, Special Publications*, *401*(1), 327–356.
- 741 Hashimoto, G. L., Roos-Serote, M., Sugita, S., Gilmore, M. S., Kamp, L. W., Carl-
742 son, R. W., & Baines, K. H. (2008). Felsic highland crust on Venus suggested
743 by Galileo near-infrared mapping spectrometer data. *Journal of Geophysical*
744 *Research: Planets*, *113*(E5).
- 745 Hasterok, D., Halpin, J. A., Collins, A. S., Hand, M., Kreemer, C., Gard, M. G., &
746 Glorie, S. (2022). New maps of global geological provinces and tectonic plates.
747 *Earth-Science Reviews*, *231*, 104069.
- 748 Head, J. W. (1990). Venus trough-and-ridge tessera: Analog to Earth oceanic crust
749 formed at spreading centers? *Journal of Geophysical Research: Solid Earth*,
750 *95*(B5), 7119–7132.
- 751 Herrick, R. R., & Hensley, S. (2023). Surface changes observed on a Venusian vol-
752 cano during the Magellan mission. *Science*, *379*(6638), 1205–1208. doi: 10
753 .1126/science.abm7735
- 754 Houston, H. (2015). 4.13 - Deep Earthquakes. In G. Schubert (Ed.), *Treatise on geo-*
755 *physics* (Second ed., p. 329 - 354). Oxford: Elsevier. Retrieved from [http://](http://www.sciencedirect.com/science/article/pii/B9780444538024000798)
756 www.sciencedirect.com/science/article/pii/B9780444538024000798
757 doi: <https://doi.org/10.1016/B978-0-444-53802-4.00079-8>
- 758 Hyndman, R. D., & Wang, K. (1993). Thermal constraints on the zone of major
759 thrust earthquake failure: The cascadia subduction zone. *Journal of Geophys-
760 ical Research: Solid Earth*, *98*(B2), 2039–2060.
- 761 Hyndman, R. D., Yamano, M., & Oleskevich, D. A. (1997). The seismogenic zone of
762 subduction thrust faults. *Island Arc*, *6*(3), 244–260.

- 763 Ivanov, M. A., & Head, J. W. (2011). Global geological map of Venus. *Planetary*
764 *and Space Science*, *59*(13), 1559–1600.
- 765 James, P. B., Zuber, M. T., & Phillips, R. J. (2013). Crustal thickness and support
766 of topography on Venus. *Journal of Geophysical Research: Planets*, *118*(4),
767 859–875.
- 768 Jull, M. G., & Arkani-Hamed, J. (1995). The implications of basalt in the formation
769 and evolution of mountains on Venus. *Physics of the Earth and Planetary Inte-*
770 *riors*, *89*(3-4), 163–175.
- 771 Jung, H., Green II, H. W., & Dobrzhinetskaya, L. F. (2004). Intermediate-depth
772 earthquake faulting by dehydration embrittlement with negative volume
773 change. *Nature*, *428*(6982), 545–549.
- 774 Jurdy, D. M., & Stoddard, P. R. (2007, 01). The coronae of Venus: Impact, plume,
775 or other origin? In *Plates, Plumes and Planetary Processes*. Geological Society
776 of America. doi: 10.1130/2007.2430(40)
- 777 Karato, S.-i., & Barbot, S. (2018). Dynamics of fault motion and the origin of con-
778 trasting tectonic style between Earth and Venus. *Scientific Reports*, *8*(1), 1–
779 11.
- 780 Kiefer, W. S., & Swafford, L. C. (2006). Topographic analysis of Devana Chasma,
781 Venus: Implications for rift system segmentation and propagation. *Journal of*
782 *structural geology*, *28*(12), 2144–2155.
- 783 Kremic, T., Ghail, R., Gilmore, M., Hunter, G., Kiefer, W., Limaye, S., . . . Wilson,
784 C. (2020). Long-duration Venus lander for seismic and atmospheric science.
785 *Planetary and space science*, *190*, 104961. doi: [https://doi.org/10.1016/](https://doi.org/10.1016/j.pss.2020.104961)
786 [j.pss.2020.104961](https://doi.org/10.1016/j.pss.2020.104961)
- 787 Krishnamoorthy, S., & Bowman, D. C. (2023). A “Floatilla” of Airborne Seismome-
788 ters for Venus. *Geophysical Research Letters*, *50*(2), e2022GL100978.
- 789 Krishnamoorthy, S., Komjathy, A., Cutts, J. A., Lognonne, P., Garcia, R. F., Pan-
790 ning, M. P., . . . others (2020). *Seismology on Venus with infrasound obser-*
791 *vations from balloon and orbit* (Tech. Rep.). Sandia National Lab.(SNL-NM),
792 Albuquerque, NM (United States).
- 793 Kryuchkov, V. (1990). Ridge belts: Are they compressional or extensional struc-
794 tures? *Earth, Moon, and Planets*, *50*(1), 471–491.
- 795 Ksanfomaliti, L., Zubkova, V., Morozov, N., & Petrova, E. (1982). Microseisms at
796 the VENERA-13 and VENERA-14 Landing Sites. *Soviet Astronomy Letters*,
797 *8*, 241.
- 798 Lenardic, A., Jellinek, A., & Moresi, L.-N. (2008). A climate induced transition in
799 the tectonic style of a terrestrial planet. *Earth and Planetary Science Letters*,
800 *271*(1-4), 34–42.
- 801 Lorenz, R. D. (2012). Planetary seismology—Expectations for lander and wind noise
802 with application to Venus. *Planetary and Space Science*, *62*(1), 86–96.
- 803 Lourenço, D. L., Rozel, A. B., Ballmer, M. D., & Tackley, P. J. (2020). Plutonic-
804 squishy lid: a new global tectonic regime generated by intrusive magma-
805 tism on Earth-like planets. *Geochemistry, Geophysics, Geosystems*, *21*(4),
806 e2019GC008756.
- 807 Maia, J. S., & Wiczorek, M. A. (2022). Lithospheric Structure of Venusian Crustal
808 Plateaus. *Journal of Geophysical Research: Planets*, e2021JE007004.
- 809 Marcq, E., Bertaux, J.-L., Montmessin, F., & Belyaev, D. (2013). Variations of
810 sulphur dioxide at the cloud top of Venus’s dynamic atmosphere. *Nature geo-*
811 *science*, *6*(1), 25–28. doi: <https://doi.org/10.1038/ngeo1650>
- 812 McGill, G. E., Steenstrup, S. J., Barton, C., & Ford, P. G. (1981). Continental
813 rifting and the origin of beta regio, Venus. *Geophysical Research Letters*, *8*(7),
814 737–740.
- 815 McKenzie, D., Jackson, J., & Priestley, K. (2005). Thermal structure of oceanic and
816 continental lithosphere. *Earth and Planetary Science Letters*, *233*(3-4), 337–
817 349.

- 818 McKinnon, W. B., Zahnle, K. J., Ivanov, B. A., & Melosh, H. (1997). Cratering on
819 Venus: Models and observations. *Venus II: Geology, geophysics, atmosphere,
820 and solar wind environment*, 969.
- 821 Mueller, N., Helbert, J., Hashimoto, G., Tsang, C. C., Erard, S., Piccioni, G., &
822 Drossart, P. (2008). Venus surface thermal emission at 1 μm in VIRTIS imag-
823 ing observations: Evidence for variation of crust and mantle differentiation
824 conditions. *Journal of Geophysical Research: Planets*, 113(E5).
- 825 Nakamura, Y., Latham, G. V., & Dorman, H. J. (1982). Apollo lunar seismic experi-
826 ment—Final summary. *Journal of Geophysical Research: Solid Earth*, 87(S01),
827 A117–A123.
- 828 Namiki, N., & Solomon, S. C. (1998). Volcanic degassing of argon and helium and
829 the history of crustal production on venus. *Journal of Geophysical Research:
830 Planets*, 103(E2), 3655–3677.
- 831 Nikolaeva, O., Ivanov, M., & Borozdin, V. (1992). Evidence on the crustal di-
832 chotomy. *Venus Geology, Geochemistry, and Geophysics-Research results from
833 the USSR*, 129–139.
- 834 O'Rourke, J., Wilson, C., Borrelli, M., Byrne, P. K., Dumoulin, C., Ghail, R., ...
835 Westall, F. (2023). Venus, the Planet: Introduction to the Evolution of Earth's
836 Sister Planet. *Space Science Reviews*, 219(10).
- 837 Pavri, B., Head III, J. W., Klose, K. B., & Wilson, L. (1992). Steep-sided domes on
838 Venus: Characteristics, geologic setting, and eruption conditions from Magellan
839 data. *Journal of Geophysical Research: Planets*, 97(E8), 13445–13478.
- 840 Peacock, S. M., & Hyndman, R. D. (1999). Hydrous minerals in the mantle wedge
841 and the maximum depth of subduction thrust earthquakes. *Geophysical Re-
842 search Letters*, 26(16), 2517–2520.
- 843 Phillips, R., Kaula, W., McGill, G., & Malin, M. (1981). Tectonics and evolution of
844 venus. *Science*, 212(4497), 879–887.
- 845 Phillips, R. J., & Malin, M. C. (1984). Tectonics of venus. *Annual Review of Earth
846 and Planetary Sciences*, 12(1), 411–443.
- 847 Price, M., & Suppe, J. (1995). Constraints on the resurfacing history of Venus from
848 the hypsometry and distribution of volcanism, tectonism, and impact craters.
849 *Earth, Moon, and Planets*, 71(1-2), 99–145.
- 850 Price, M., Watson, G., Suppe, J., & Brankman, C. (1996). Dating volcanism and
851 rifting on Venus using impact crater densities. *Journal of Geophysical Re-
852 search: Planets*, 101(E2), 4657–4671.
- 853 Regorda, A., Thieulot, C., Van Zelst, I., Erdős, Z., Maia, J., & Buitert, S. (2023).
854 Rifting Venus: insights from numerical modeling. *Journal of Geophysical
855 Research: Planets*, 128(3), e2022JE007588. doi: 10.1029/2022JE007588
- 856 Richards, F., Hoggard, M., Cowton, L., & White, N. (2018). Reassessing the ther-
857 mal structure of oceanic lithosphere with revised global inventories of basement
858 depths and heat flow measurements. *Journal of Geophysical Research: Solid
859 Earth*, 123(10), 9136–9161.
- 860 Rolf, T., Weller, M., Gülcher, A., Byrne, P., O'Rourke, J. G., Herrick, R., ... others
861 (2022). Dynamics and evolution of Venus' mantle through time. *Space Science
862 Reviews*, 218(8), 70.
- 863 Romeo, I., & Capote, R. (2011). Tectonic evolution of Ovda Regio: An example
864 of highly deformed continental crust on Venus? *Planetary and Space Science*,
865 59(13), 1428–1445.
- 866 Romeo, I., & Turcotte, D. (2008). Pulsating continents on Venus: An explanation
867 for crustal plateaus and tessera terrains. *Earth and Planetary Science Letters*,
868 276(1-2), 85–97. Retrieved from <https://doi.org/10.1016/j.epsl.2008.09.009>
869 doi: 10.1016/j.epsl.2008.09.009
- 870 Sabbeth, L., Smrekar, S., & Stock, J. (2023a). Estimated seismicity of Venusian
871 wrinkle ridges based on fault scaling relationships. *Earth and Planetary Sci-
872 ence Letters*, 619, 118308. Retrieved from <https://www.sciencedirect.com/>

- 873 science/article/pii/S0012821X23003217 doi: 10.1016/j.epsl.2023.118308
 874 Sabbeth, L., Smrekar, S. E., & Stock, J. M. (2023b). Using InSight data to calibrate
 875 seismicity from remote observations of surface faulting. *Journal of Geophysical*
 876 *Research: Planets*, *128*(6), e2022JE007686. Retrieved from <https://agupubs>
 877 [.onlinelibrary.wiley.com/doi/abs/10.1029/2022JE007686](https://agupubs.onlinelibrary.wiley.com/doi/abs/10.1029/2022JE007686) doi: 10.1029/
 878 2022JE007686
- 879 Salvador, A., Avice, G., Breuer, D., Gillmann, C., Jacobson, S., Lammer, H., ...
 880 others (2022). Magma ocean, water, and the early atmosphere of venus. *Space*
 881 *Sci Rev.*
- 882 Scholz, C. H. (2019). *The mechanics of earthquakes and faulting*. Cambridge univer-
 883 sity press.
- 884 Seno, T. (2009). Determination of the pore fluid pressure ratio at seismogenic
 885 megathrusts in subduction zones: Implications for strength of asperities and
 886 Andean-type mountain building. *Journal of Geophysical Research: Solid Earth*,
 887 *114*(B5).
- 888 Seton, M., Müller, R. D., Zahirovic, S., Williams, S., Wright, N. M., Cannon, J., ...
 889 McGirr, R. (2020). A global data set of present-day oceanic crustal age and
 890 seafloor spreading parameters. *Geochemistry, Geophysics, Geosystems*, *21*(10),
 891 e2020GC009214.
- 892 Smrekar, S. E., Davaille, A., & Sotin, C. (2018). Venus interior structure and dy-
 893 namics. *Space Science Reviews*, *214*(5), 1–34.
- 894 Smrekar, S. E., Dyar, D., Helbert, J., Hensley, S., Nunes, D., & Whitten, J. (2020).
 895 VERITAS (Venus Emissivity, Radio Science, InSAR, Topography, and Spec-
 896 troscopy): A proposed Discovery mission. In *European planetary science*
 897 *congress* (p. EPSC2020-447). doi: <https://doi.org/10.5194/epsc2020-447>
- 898 Smrekar, S. E., Ostberg, C., & O'Rourke, J. G. (2023). Earth-like lithospheric thick-
 899 ness and heat flow on Venus consistent with active rifting. *Nature Geoscience*,
 900 *16*(1), 13–18.
- 901 Smrekar, S. E., & Sotin, C. (2012). Constraints on mantle plumes on venus: Implica-
 902 tions for volatile history. *Icarus*, *217*(2), 510–523.
- 903 Smrekar, S. E., & Stofan, E. R. (1997). Corona formation and heat loss on venus by
 904 coupled upwelling and delamination. *Science*, *277*(5330), 1289–1294.
- 905 Smrekar, S. E., Stofan, E. R., Mueller, N., Treiman, A., Elkins-Tanton, L., Helbert,
 906 J., ... Drossart, P. (2010). Recent hotspot volcanism on Venus from VIRTIS
 907 emissivity data. *Science*, *328*(5978), 605–608. doi: [https://doi.org/10.1126/](https://doi.org/10.1126/science.1186785)
 908 [science.1186785](https://doi.org/10.1126/science.1186785)
- 909 Solomon, S. (1993). The geophysics of venus. *Physics Today*, *46*(7), 48–55.
- 910 Stevenson, D. J., Cutts, J. A., Mimoun, D., Arrowsmith, S., Banerdt, W. B., Blom,
 911 P., ... others (2015). Probing the interior structure of Venus.
- 912 Stoddard, P. R., & Jurdy, D. M. (2012). Topographic comparisons of uplift fea-
 913 tures on Venus and Earth: Implications for Venus tectonics. *Icarus*, *217*(2),
 914 524–533.
- 915 Strom, R. G., Schaber, G. G., & Dawson, D. D. (1994). The global resurfacing of
 916 Venus. *Journal of Geophysical Research: Planets (1991–2012)*, *99*(E5), 10899–
 917 10926.
- 918 Tian, Y., Herrick, R. R., West, M. E., & Kremic, T. (2023). Mitigating Power and
 919 Memory Constraints on a Venusian Seismometer. *Seismological Society of*
 920 *America*, *94*(1), 159–171.
- 921 Tichelaar, B. W., & Ruff, L. J. (1993). Depth of seismic coupling along subduction
 922 zones. *Journal of Geophysical Research: Solid Earth*, *98*(B2), 2017–2037.
- 923 van Dinther, Y., Gerya, T. V., Dalguer, L. A., Corbi, F., Funicello, F., & Mai,
 924 P. M. (2013). The seismic cycle at subduction thrusts: 2. Dynamic implica-
 925 tions of geodynamic simulations validated with laboratory models. *Journal of*
 926 *Geophysical Research: Solid Earth*, *118*(4), 1502–1525.
- 927 van Dinther, Y., Gerya, T. V., Dalguer, L. A., Mai, P. M., Morra, G., & Giardini,

- 928 D. (2013). The seismic cycle at subduction thrusts: Insights from seismo-
929 thermo-mechanical models. *Journal of Geophysical Research: Solid Earth*,
930 *118*(12), 6183–6202.
- 931 van Dinther, Y., Mai, P. M., Dalguer, L. A., & Gerya, T. V. (2014). Modeling the
932 seismic cycle in subduction zones: The role and spatiotemporal occurrence of
933 off-megathrust earthquakes. *Geophysical Research Letters*, *41*(4), 1194–1201.
- 934 Van Zelst, I. (2022). Comment on “Estimates on the frequency of volcanic eruptions
935 on Venus” by Byrne & Krishnamoorthy (2022). *Journal of Geophysical*
936 *Research: Planets*, *127*(12), e2022JE007448. doi: 10.1029/2022JE007448
- 937 Van Zelst, I., Wollherr, S., Gabriel, A.-A., Madden, E. H., & van Dinther, Y. (2019).
938 Modeling megathrust earthquakes across scales: one-way coupling from geo-
939 dynamics and seismic cycles to dynamic rupture. *Journal of Geophysical*
940 *Research: Solid Earth*, *124*(11), 11414–11446. doi: 10.1029/2019JB017539
- 941 Wang, J., Zhao, D., & Yao, Z. (2017). Seismic anisotropy evidence for dehydration
942 embrittlement triggering intermediate-depth earthquakes. *Scientific reports*,
943 *7*(1), 1–9.
- 944 Weller, M., Lenardic, A., & O’Neill, C. (2015). The effects of internal heating and
945 large scale climate variations on tectonic bi-stability in terrestrial planets.
946 *Earth and Planetary Science Letters*, *420*, 85–94.
- 947 Wright, T. J., Elliott, J. R., Wang, H., & Ryder, I. (2013). Earthquake cycle defor-
948 mation and the Moho: Implications for the rheology of continental lithosphere.
949 *Tectonophysics*, *609*, 504–523.
- 950 Zuber, M. (1990). Ridge belts: Evidence for regional-and local-scale deformation on
951 the surface of venus. *Geophysical Research Letters*, *17*(9), 1369–1372.